



TITLE:

A NUMERICAL EXPERIMENT OF EFFECTS OF TURBULENT TRANSFER PROCESSES ON THE LAND AND SEA BREEZE

AUTHOR(S):

YOSHIKADO, Hiroshi; ASAI, Tomio

CITATION:

YOSHIKADO, Hiroshi ...[et al]. A NUMERICAL EXPERIMENT OF EFFECTS OF TURBULENT TRANSFER PROCESSES ON THE LAND AND SEA BREEZE. Contributions of the Geophysical Institute, Kyoto University 1972, 12: 33-48

ISSUE DATE:

1972-12

URL:

<http://hdl.handle.net/2433/178620>

RIGHT:

A NUMERICAL EXPERIMENT OF EFFECTS OF TURBULENT TRANSFER PROCESSES ON THE LAND AND SEA BREEZE

By

Hiroshi YOSHIKADO and Tomio ASAI

(Received September 8, 1972)

Abstract

A two-dimensional land and sea breeze model was integrated numerically for some different formulae of vertical turbulent exchanges of heat and momentum in order to examine the effect of the formulations on land and sea breeze circulation. For the upper boundary layer the use of a formula of turbulent exchange coefficient K to be locally estimated by the thermal stratification and the vertical wind shear yields an extremely weak land and sea breeze. The formula of K used by Estoque [1961] which takes into consideration the Richardson number of the surface layer gives some characteristic features of the land and sea breeze. It is suggested that the effect of so-called penetrative convection should be taken into account in turbulent transfer processes.

1. Introduction

The land and sea breeze circulation is one of transient phenomena in the atmospheric boundary layer. Because of a thermal contrast of the underlying inhomogeneous surface, the corresponding horizontal gradient of temperature arises in the lower atmosphere and generates a diurnal variation of the land and sea breeze in coastal regions. A typical horizontal scale of the breeze is known to be tens of kilometers in middle latitudes. It should also be remarked as general features that the sea breeze can be observed very clearly but that the land breeze is much weaker, and that above several hundred meters there is a counter flow layer thicker and weaker than the lower primary flow.

Concerning the sea breeze theory, the linearized models by Schmidt [1947], Haurwitz [1947], Defant [1950] and others established the basic mechanisms of the sea breeze, *i. e.* the effects carried by the thermal contrast of the land and the sea, the Coriolis acceleration and the internal friction.

In the last decade nonlinear models of the sea breeze have been developed following the progress of high speed electronic computer system and the sea breeze theory has made great strides as an example of the boundary layer flows in which the turbulent transfer of heat and momentum plays an important role. Most important is the model designed by Estoque [1961], on the basis of which a set of hydrothermodynamic equations for motions in the vertical plane perpendicular to a straight coastline were integrated with respect to time and the sea breeze circulation with a diurnal

variation was quantitatively elucidated. Estoque [1962] also investigated an influence of general flow on the sea breeze by imposing in a model identical to his previous one [1961] a geostrophically balanced initial condition and a corresponding pressure gradient at the upper boundary unchanged during the period of integration. Furthermore, using a similar numerical model containing the equations of moisture transfer and heat balance at the surface, Magata [1965] examined the effects of solar radiation, the latent heat release due to condensation and the vertical shear of the general flow. McPherson [1970] extended Estoque's model to a three-dimensional one and showed the sea breeze circulation associated with a rectangular bay.

Apart from studies on the effects of the external conditions on the sea breeze circulation, there remains another important problem to be studied on the basis of these numerical models, which is the evaluation of the turbulent transfer processes of momentum and heat in the circulation. The turbulent transfer process in the atmospheric boundary layer is an essential mechanism for inducing boundary layer phenomena such as the sea breeze. Little is known, however, about the turbulent transfer process above the surface layer under different atmospheric conditions. In Estoque's model the turbulent exchange coefficient K is prescribed to decrease linearly with height in the upper boundary layer, though it varies with time in proportion to the value of K at the top of the surface layer calculated as a function of its stability. In some other models, K is assumed to be constant in time and in space. It is, however, desirable to estimate K based on a more physical foundation of the sub-grid scale turbulence, since it plays a significant role in reflecting the land-sea thermal contrast on the lower atmosphere. In this paper a series of numerical experiments is performed using a sea breeze model similar to Estoque's with some formulations of turbulent transfer respectively to clarify what effect each of these formulations has in a land and sea breeze model.

2. Model and basic equations

Let us consider a land and sea breeze circulation in a vertical plane perpendicular to a straight coast-line, which is essentially the same as Estoque's [1961].

A Cartesian coordinate system is used in which the x axis is normal to the coast-line, the y axis is along to it and the z axis is vertically upward. The domain considered is bounded by $x = \pm D$, $z = H$ and $z = 0$ which stands for the sea surface ($x < 0$) and the land surface ($x \geq 0$). The atmospheric layer is divided into two sublayers: the surface layer up to the height of $z = h$ in which the vertical turbulent fluxes of heat and momentum are assumed to be constant and the transition layer above the surface layer, as shown in Fig. 1.

For the surface layer hold the following equations.

$$\frac{\partial}{\partial z} \left(K \frac{\partial U}{\partial z} \right) = 0, \quad (1)$$

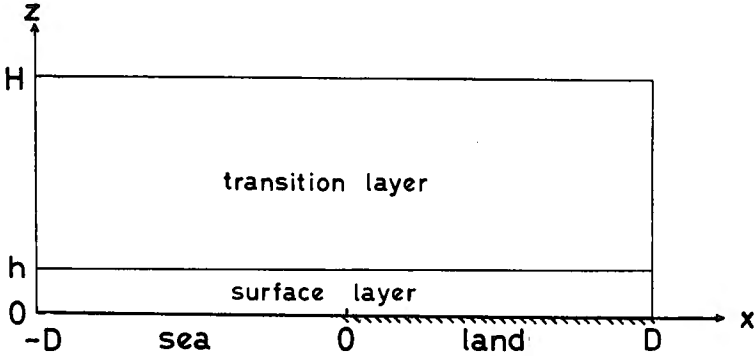


Fig. 1. The coordinate system of the model.

$$\frac{\partial}{\partial z} \left(K \frac{\partial \theta}{\partial z} \right) = 0, \tag{2}$$

where U is the horizontal wind velocity whose direction is constant in this layer and θ is the potential temperature. The turbulent exchange coefficient K is described in the next section as well as that for the upper sublayer.

The basic equations for the transition layer are as follows.

$$\frac{\partial u}{\partial t} + u \frac{\partial u}{\partial x} + w \frac{\partial u}{\partial z} = -C_p \theta \frac{\partial \pi^*}{\partial x} + \frac{\partial}{\partial z} \left(K \frac{\partial u}{\partial z} \right) + f v + K_{hor} \frac{\partial^2 u}{\partial x^2}, \tag{3}$$

$$\frac{\partial v}{\partial t} + u \frac{\partial v}{\partial x} + w \frac{\partial v}{\partial z} = \frac{\partial}{\partial z} \left(K \frac{\partial v}{\partial z} \right) - f u + K_{hor} \frac{\partial^2 v}{\partial x^2}, \tag{4}$$

$$\frac{\partial \theta}{\partial t} + u \frac{\partial \theta}{\partial x} + w \frac{\partial \theta}{\partial z} = \frac{\partial}{\partial z} \left(K \frac{\partial \theta}{\partial z} \right) + K_{hor} \frac{\partial^2 \theta}{\partial x^2}, \tag{5}$$

$$\frac{\partial \pi^*}{\partial z} = -\frac{g}{C_p \theta}, \tag{6}$$

$$\frac{\partial^2 w}{\partial z^2} = -\frac{\partial}{\partial z} \left(\frac{\partial u}{\partial z} \right), \tag{7}$$

where u, v and w represent the x, y and z components of the wind velocity respectively, $\pi^* = T/\theta$ stands for the pressure, T is the temperature, K_{hor} is the horizontal turbulent exchange coefficient and other symbols have their customary meanings. Eq.(6) indicates the hydrostatic balance, which may be well satisfied considering the scale of the phenomenon concerned here, that is vertically a few kilometers and horizontally tens of kilometers. Eq.(7) is the continuity equation differentiated with z . This does not necessarily satisfy the mass conservation exactly, and it is questionable how

serious errors may be included in the calculated wind and temperature. However, as far as mass conservation itself is not discussed, the errors which might be caused by a violation of the mass conservation law may be considered not so critical (*see* Neumann and Mahrer [1971]).

The boundary conditions for the foregoing set of equations are

$$\frac{\partial}{\partial x}(u, v, \theta) = 0 \quad \text{at } x = \pm D, \quad (8)$$

$$U = w = 0, \quad T(^{\circ}K) = \begin{cases} 283 & \text{for } x < 0, \\ 283 + 10 \sin \frac{t-8}{12} \pi & \text{for } x \geq 0, \end{cases} \quad \text{at } z = 0, \quad (9)$$

$$u = v = w = 0, \quad \theta = \theta_H = \text{const.},$$

$$\text{and } \pi^* = \pi_H^* = \text{const.} \quad \text{at } z = H. \quad (10)$$

At the level of $z=h$, the horizontal wind velocity, the potential temperature and their vertical gradients are assumed to be continuous except for one case which will be mentioned later. The difference between the land and the sea is embodied only in the condition for the surface temperature.

An initial condition has lesser significance because numerical time integrations are expected to lead finally to a definite state indifferent to the initial condition for a given boundary condition. The initial conditions used are

$$u = v = w = 0, \quad \frac{\partial \theta}{\partial x} = \frac{\partial \theta}{\partial y} = \frac{\partial \pi^*}{\partial x} = \frac{\partial \pi^*}{\partial y} = 0, \quad (11)$$

except Case 1 to be mentioned later, in which $u = -1 \text{ m sec}^{-1}$ is assumed.

Eqs. (3)–(7) are transformed to a commonly used set of finite difference equations and solved numerically, while Eqs. (1) and (2) are solved analytically. A centered finite difference scheme is used and the grid system is shown in Table 1.

Table 1. Grid system

x (km)	z (m)
0	0
± 1	46 (h)
± 3	100
± 7	215
± 15	464
± 31	1000
± 63	2150
± 127 (D)	4640 (H)

Constants adopted in the present calculations are as follows.

$$\begin{aligned}
 C_p &= 1.004 \times 10^7 \quad \text{erg gr}^{-1}\text{deg}^{-1}, \\
 g &= 980.0 \quad \text{cm sec}^{-2}, \\
 f &= 8.365 \times 10^{-5} \quad \text{sec}^{-1} \quad (\phi = 35^\circ\text{N}), \\
 k_0 &= 0.4, \\
 \theta_H &= 296.43 \quad ^\circ\text{K}, \\
 \pi_H^* &= 0.84933 \quad (p_H = 564.6\text{mb}), \\
 K_{hor} &= 10^4 \quad \text{m}^2\text{sec}^{-1}.
 \end{aligned}$$

The initial time when the entire domain is horizontally uniform is taken at 0800 LST.

3. Different representations of turbulent exchange

Numerical experiments are carried out by making use of different formulae of turbulent exchange successively in the governing equations. It is assumed here that the turbulent exchange coefficient of momentum is equivalent to that of heat.

Case 1

For the surface layer,

$$\begin{aligned}
 \tau &= \rho C_D U_h^2, \\
 Q &= -\rho C_p C_D U_h (\theta_h - \theta_0),
 \end{aligned} \tag{12}$$

where τ and Q are the vertical fluxes of momentum and heat respectively, and the subscripts of U and θ represent the respective levels at which the variables are defined. The drag coefficient C_D is specified to be 0.0022 everywhere. In the second case C_D is assumed to be 0.01 for the land and 0.001 for the sea, which is identified as Case 1'.

The so-called bulk method which is often applied to large-scale circulation models is intended to be examined here. For simplicity a moderate constant value of K which is $10 \text{ m}^2 \text{ sec}^{-1}$ is adopted for the transition layer.

Case 2

Different formulae of K in the transition layer are adopted for Cases 2-4, in all of which the formula used by Estoque [1963] is applied to the surface layer. The turbulent exchange coefficient for the surface layer is given as follows.

$$K = \begin{cases} 0.9 \left(\frac{g}{\bar{\theta}} \left| \frac{\partial \theta}{\partial z} \right| \right)^{1/2} (z + z_0), & Ri_m < -0.03 \\ [k_0(z + z_0)(1 + \alpha Ri)]^2 \frac{\partial U}{\partial z}, & -0.03 \leq Ri_m \leq \left| \frac{1}{\alpha} \right| \\ K_{min}, & Ri_m > \left| \frac{1}{\alpha} \right| \end{cases} \quad (13)$$

where, $Ri_m = \frac{g}{\bar{\theta}} \frac{\theta_{h+\Delta z} - \theta_0}{U_{h+\Delta z}} (h + \Delta z)$, in which $(h + \Delta z)$ indicates the grid point adjacent above the level h . K is bounded by a minimum value $K_{min} = 1 \text{ m}^2 \text{ sec}^{-1}$. $\alpha = -3$ is an empirical constant and roughness length z_0 is specified to be 1 cm. $\bar{\theta}$ is the potential temperature averaged vertically in the corresponding layer. The wind velocity and the temperature at the level h are calculated by making use of the conditions at the level h mentioned in the preceding section and the assumption that the wind direction below the level $(h + \Delta z)$ is constant.

For the transition layer,

$$K = \frac{H-z}{H-h} K_h. \quad (14)$$

This is the same that Estoque [1961, 1962, 1963] used in his numerical model.

Case 3

For the transition layer,

$$K = \left(\frac{H-z}{H-h} \right)^2 \left[K_h + (z-h) \left\{ \left(\frac{\partial K}{\partial z} \right)_h + \frac{2K_h}{H-h} \right\} \right] \quad (15)$$

This cubic polynomial distribution of K follows O'Brien [1970] who proposed this formula to take into account the physical requirement that the K distribution and its first derivative are to be continuous with height. Also, K suggested by some observations seems to reach a maximum value at a few hundred meter height and to diminish upward (see e.g. Zilitinkevich *et al.* [1967]).

The upper boundary in the present model is so high that Eq. (15) gives too large a maximum value of K at a level higher than 1000 m. Hence Eq. (15) is applied to the layer confined up to the grid level next to the upper boundary, *i.e.* about 2000 m height, and a small constant value of K , $1 \text{ m}^2 \text{ sec}^{-1}$, is given above the level.

Case 4

$$K = \begin{cases} l^2 \left| \frac{\partial U}{\partial z} \right| (1 - \alpha S), & \frac{\partial \theta}{\partial z} \leq 0 \\ l^2 \left| \frac{\partial U}{\partial z} \right| (1 + \alpha S)^{-1}, & \frac{\partial \theta}{\partial z} > 0 \end{cases} \quad (16)$$

where $S = \frac{(g\theta)^{1/2}}{\theta} \frac{\partial\theta/\partial z}{\partial U/\partial z}$, $l = k_0(z+z_0) / [1 + \frac{fk_0(z+z_0)}{0.00027U}]$,

$\alpha = 18$ is a numerical constant, and $K_{min} = 1 \text{ m}^2 \text{ sec}^{-1}$.

Estoque and Bhumralkar [1969] used this formula which was an extension of Blackadar's formulation [1962] for a neutral boundary layer to a thermally stratified case. In the present work this is taken tentatively as an example in which the turbulent exchange coefficient in the transition layer is related to the wind and the temperature fields at each locality.

4. Results

A numerical time integration was performed during a period of 4 days or more for each of the cases described in Section 3.

(a) *Case 1 and Case 1'*

The wind hodographs at the levels of 100 m and 1000 m over the coast-line for Case 1 are shown in Figs. 2a and b. Maximum velocities of land and sea breezes attain about 1 m sec^{-1} on the second day from the initial time. After the second day, wind velocity decreases especially at the lower level, and consequently the heat exchange at the underlying surface calculated by Eq. (12) decreases.

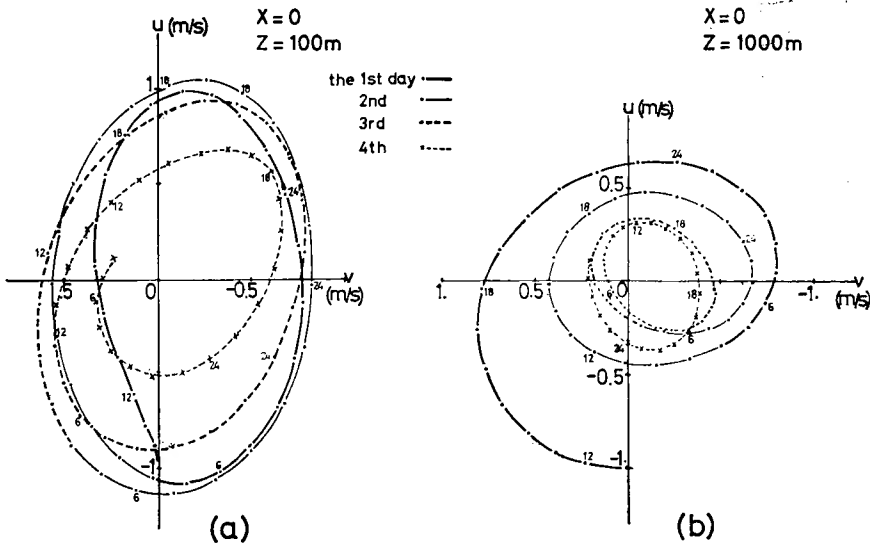


Fig. 2. The wind hodographs at the levels of (a) $z=100\text{m}$ and (b) $z=1000\text{m}$ above the coast-line for Case 1.

In Case 1', as shown in Fig. 3a, wind velocity of the land breeze is distinctly different from that of the sea breeze. The sea breeze diminishes day by day, while

the land breeze diminishes slightly. This feature is connected with the following situation. The value of C_D adopted in Case 1' is so much smaller over the sea than over the land that the flux of heat which is downward in the surface layer is smaller over the sea when averaged over one day. This results in a higher temperature in the lower portion of the transition layer over the sea than over the land, as shown in Fig. 4.

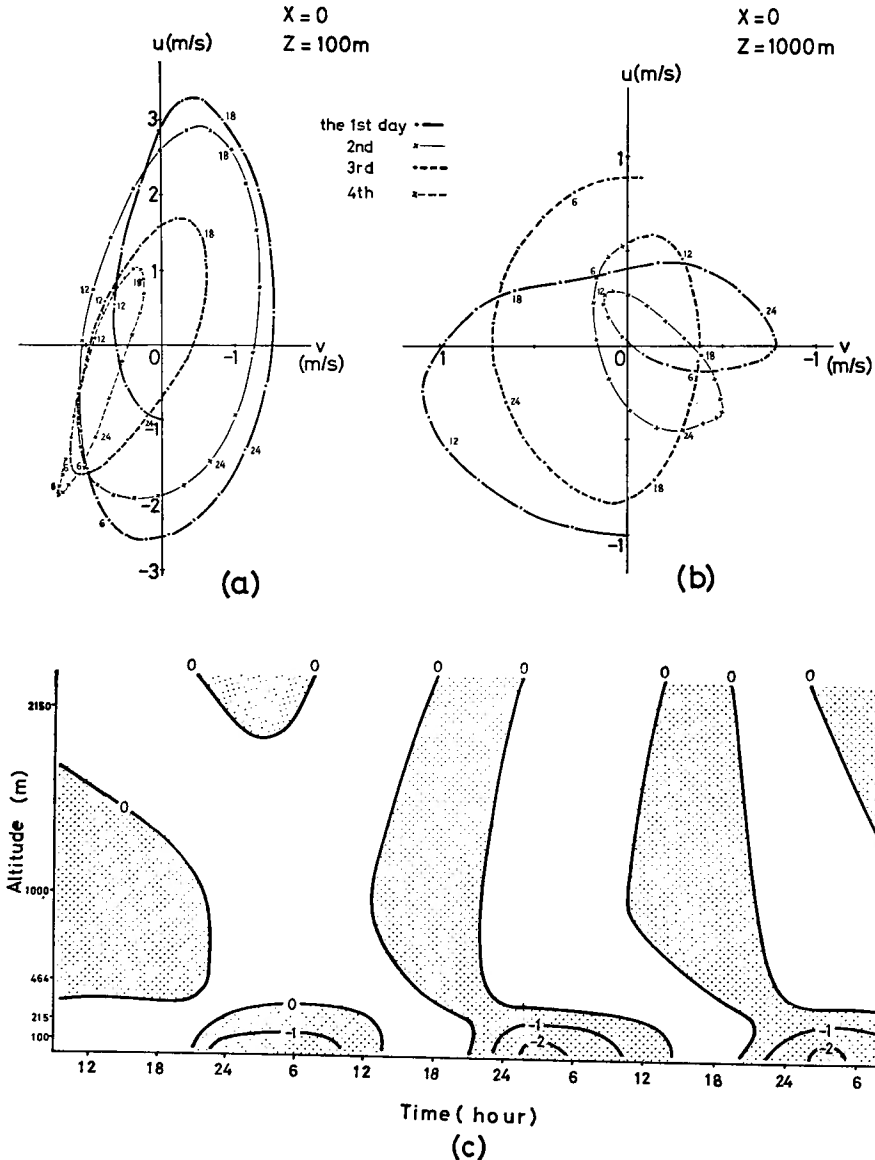


Fig. 3. (a), (b) Same as Fig. 2 but for Case 1'.
 (c) The vertical time section of u above the coast-line up to the third day for Case 1'.

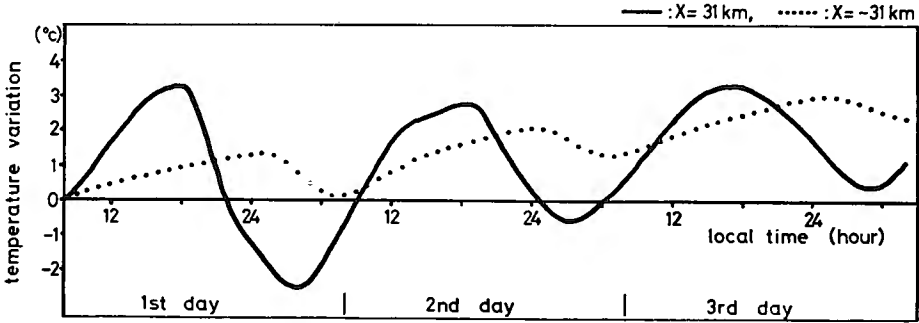


Fig. 4. The temperature variations at the level of $z=100\text{m}$ for Case 1'.

(b) Case 2 and Case 3

The vertical distributions of K for different cases are depicted in Fig. 5. The values of K for Cases 2 and 3 shown in Fig. 5 are those at 1400 LST when the thermal stratification in the surface layer above the coast-line is most unstable. The value of K in the surface layer for Case 3 is almost the same as that for Case 2, while in the lower transition layer K for Case 3 is one order greater than that for Case 2 and the contrary is true in the upper portion. At night over the land and daytime over the sea when the thermal stratification is stable K reduces to small values following Eq. (14) or (15).

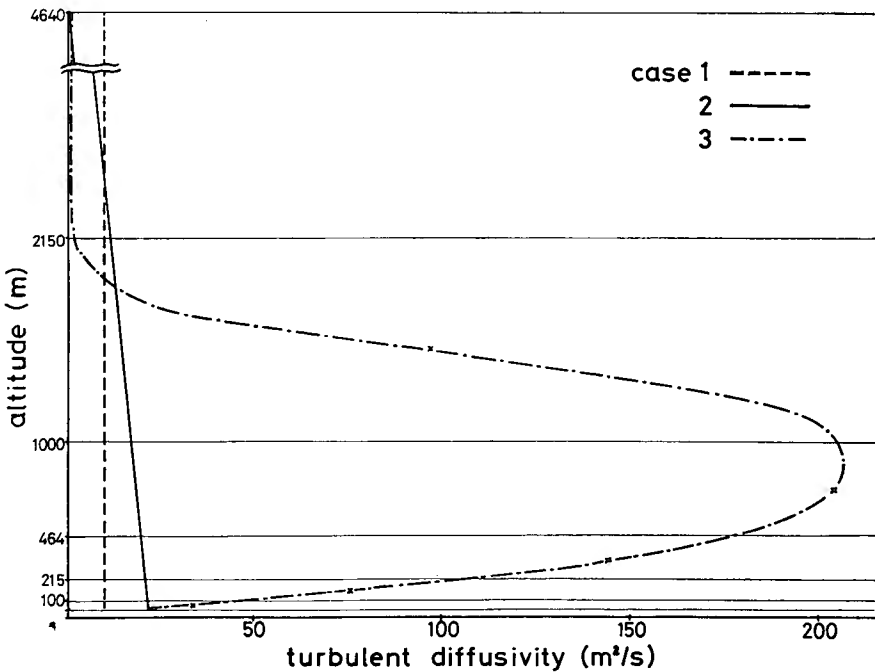


Fig. 5. Examples of the vertical distribution of K for the different cases.

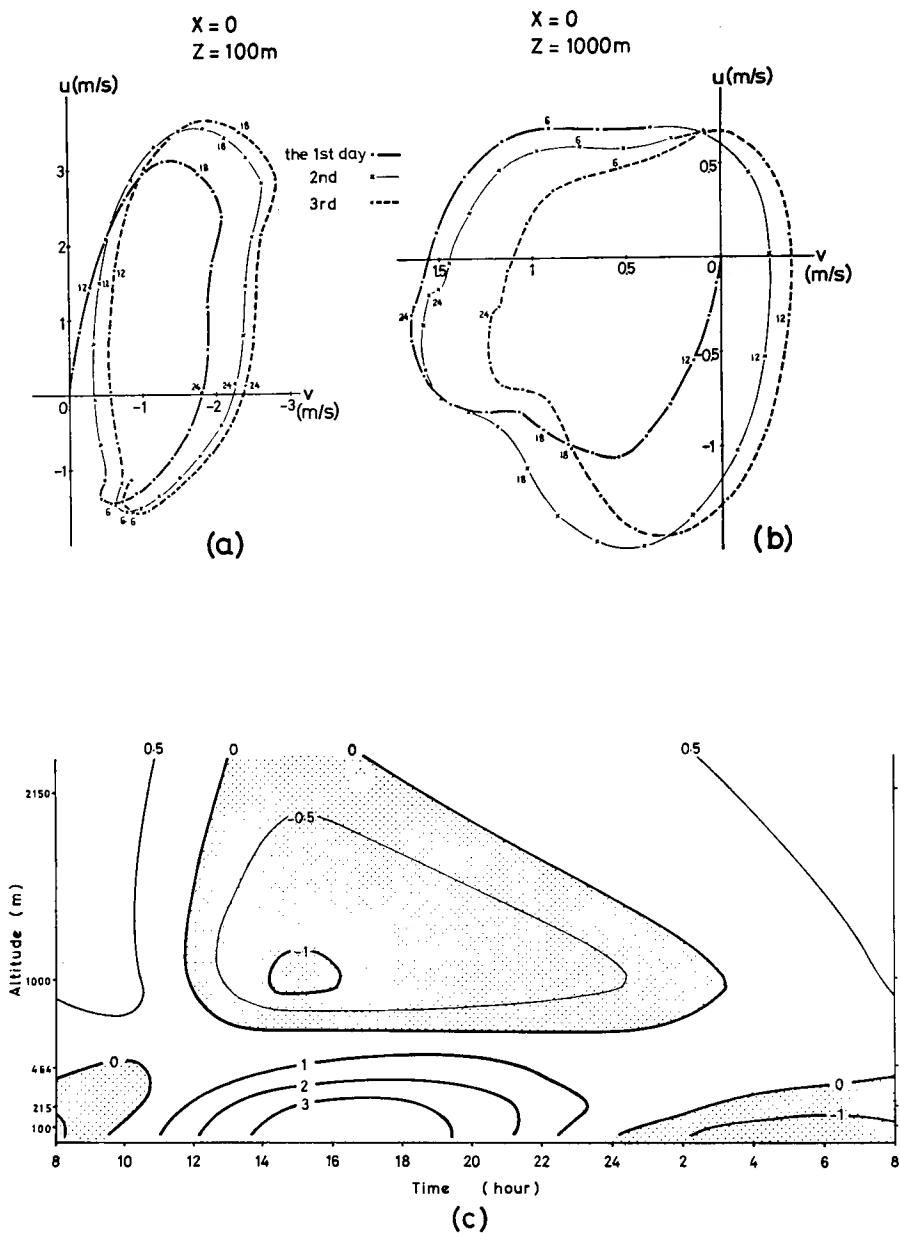


Fig. 6. The wind hodographs at the levels of (a) $z = 100\text{m}$ and (b) $z = 1000\text{m}$ above the coast-line for Case 2. No motion is assumed at the initial time. (c) The vertical time section of u above the coast-line during the sixth day for Case 2.

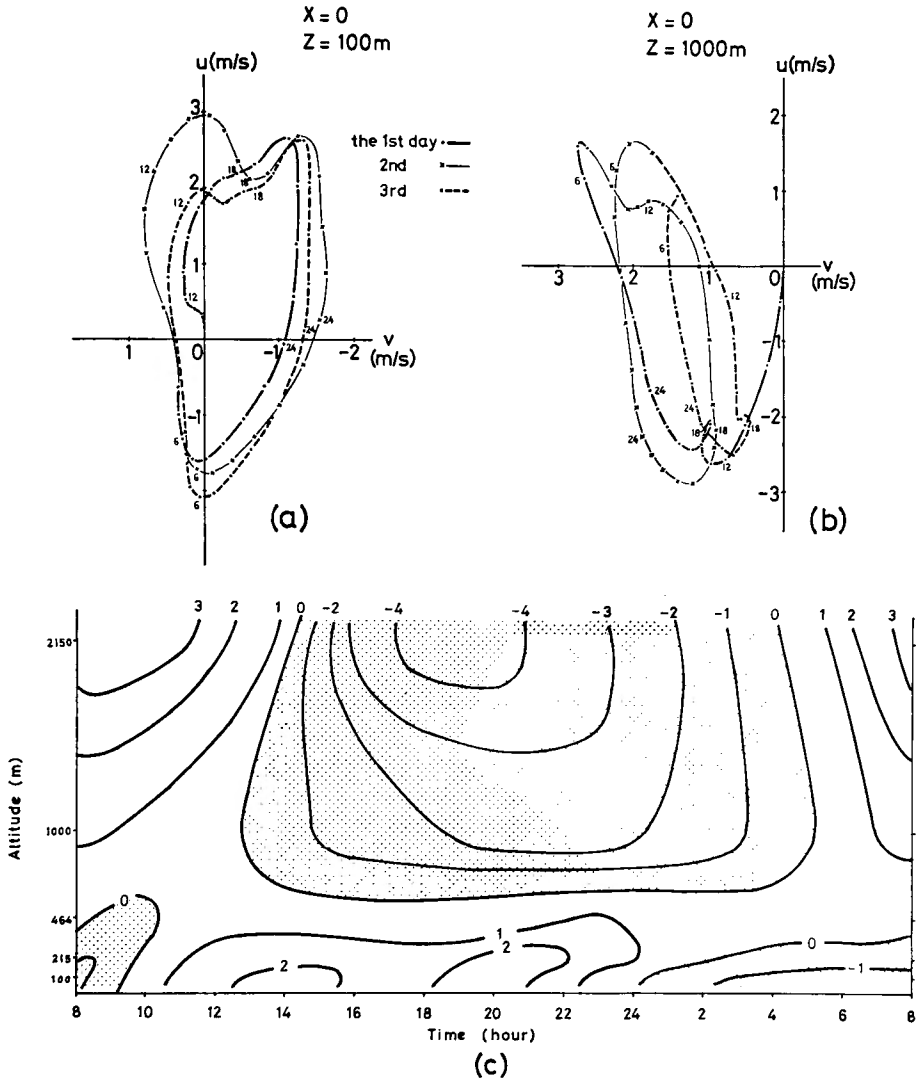


Fig. 7. Same as Fig. 6, but for Case 3

In Case 2 the circulation system tends to a stationary diurnal variation within a few days as seen in Figs. 6a and b. The vertical time section of the u component in the 6th day shows that the sea breeze lasts from 1000 to 2400 LST extending up to about 700 m height, above which is observed a weak counter flow, and the land breeze sets in after 2400 LST. In Case 3 there can be seen two features different from Case 2. One of them is the appearance of two maxima in the wind speed during the period of the sea breeze after the second day. This feature is well illustrated by Fig. 8 which is the horizontal time section of u at the height of 100 m for Cases 2 and 3.

In Case 2 it can be seen that the sea breeze forms near the coast, extends gradually and reaches a maximum 15 km inland at about 1900 LST. On the other hand in Case 3 a further development of the sea breeze is suppressed over the land during the daytime. A maximum of the sea breeze appears over the sea in the early afternoon and another maximum is observed over the land after 1800 LST. The wind hodograph above the coast-line is affected by these two maxima of the sea breeze. Less development of the sea breeze over the land during the daytime may be due to an intense turbulent exchange of momentum associated with extremely large values of

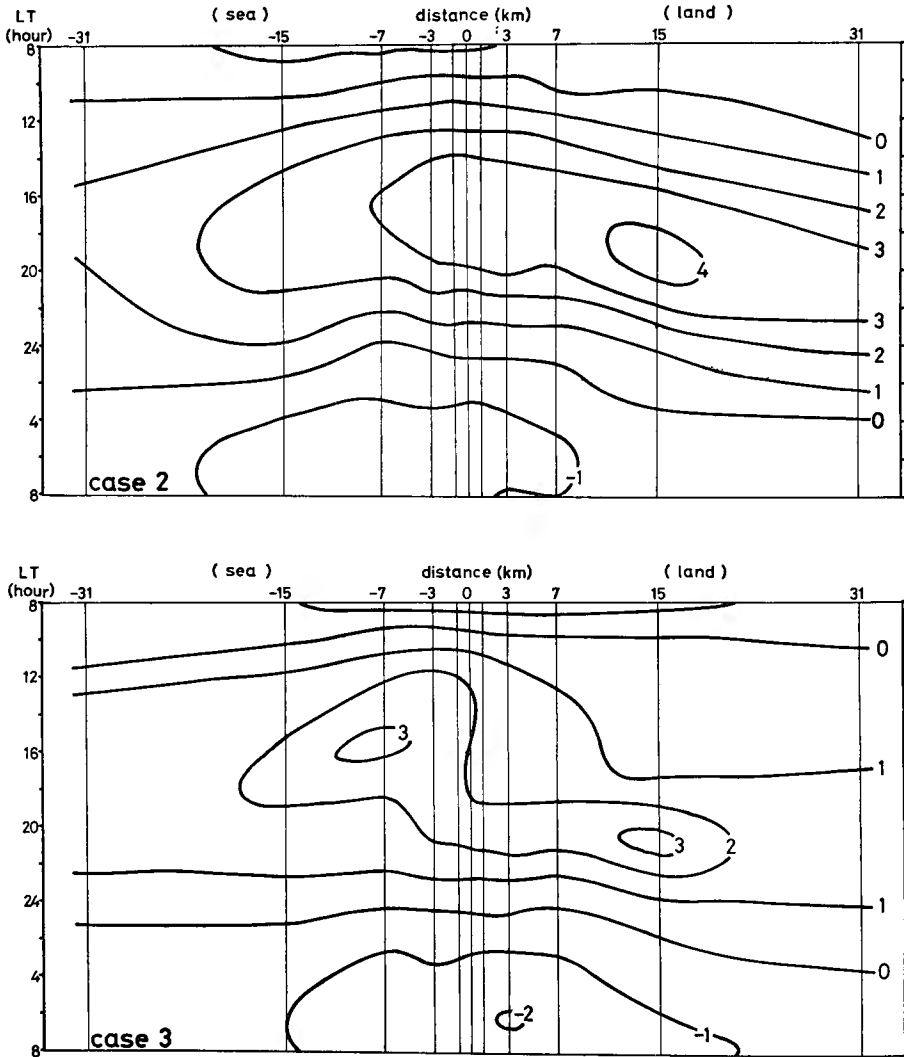


Fig. 8. The horizontal time sections of u at the level of $z=100\text{m}$ during the sixth day for Cases 2 and 3.

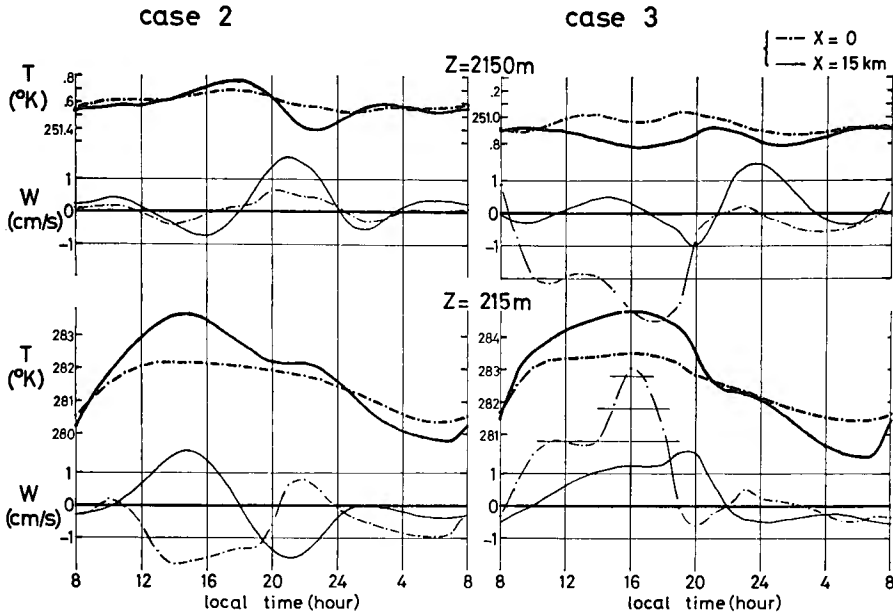


Fig. 9. Variations of the temperature and the vertical velocities during the sixth day for Cases 2 and 3.

K over the land. The second feature of Case 3 is that the counter flow in upper levels is much stronger than the respective land and sea breeze in lower levels as shown in Fig. 6c. It should also be noticed that some remarkable differences between Cases 2 and 3 can be seen in the vertical flow and the temperature fields. Fig. 9 represents variations of temperature and vertical velocity with time at four grid points which are located at a higher and a lower level over the coast-line and 15 km inland respectively for Cases 2 and 3. In Case 2 the vertical motion at the lower level above the coast-line becomes downward after 1100 LST when the sea breeze proceeds inland, while in Case 3 it is kept upward till 1900 LST and is much greater than in Case 2 as well as the downward motion at the upper level. A large horizontal gradient of temperature is found in the afternoon at the upper level in Case 3.

(c) Case 4

The values of K calculated following Eq. (16) at every time step at every grid point result in a constant as they are assumed not to be smaller than the minimum value. Figs. 10a and b are the wind hodographs for Case 4. Diurnal variations shown in Fig. 10a seem on the whole to be stationary on the third day. The used profile function derived from Eq. (13) is apt to give a larger variation of the temperature at the level of $z=h$ to a cooling under stable stratification than to a heating under unstable stratification. In other words, night cooling propagates upward more effectively than heating in the daytime. Thus the land breeze is observed fairly as strong in lower levels in spite of the smallness of K in the transition layer while the sea breeze is very weak.

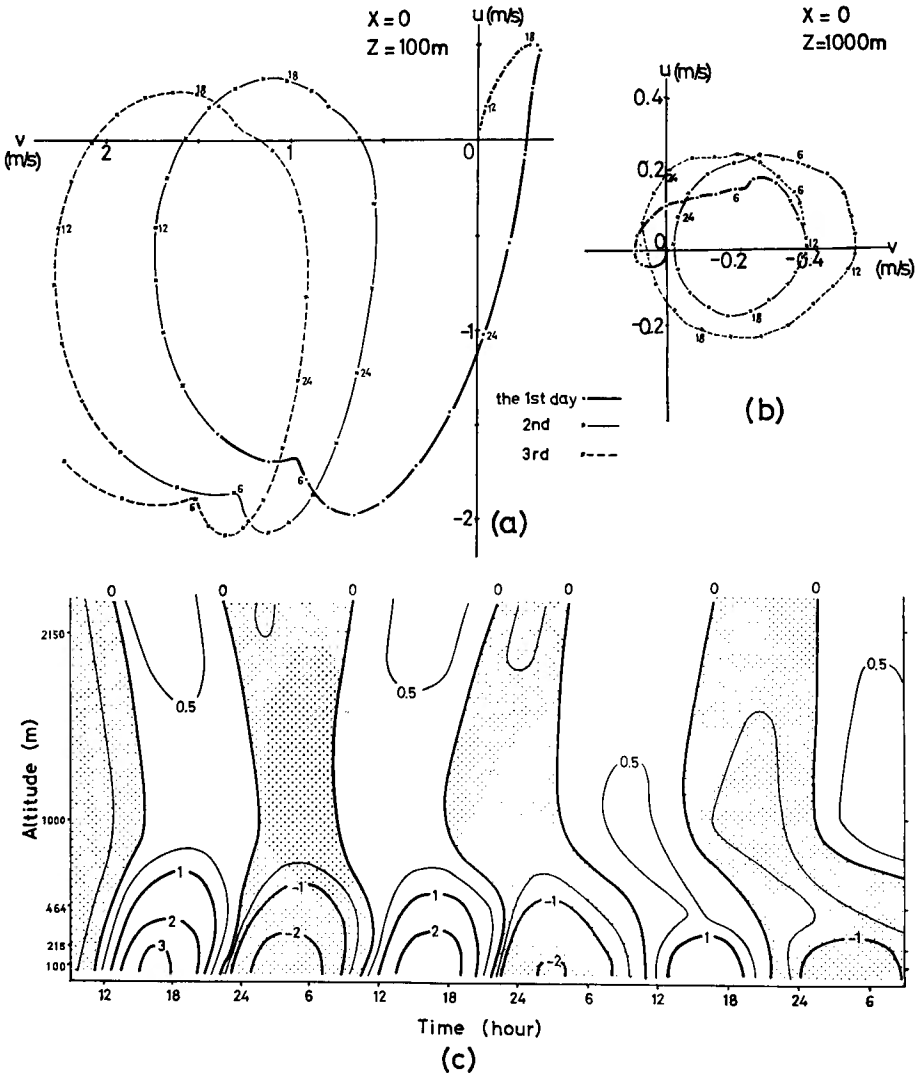


Fig. 10. Same as Fig. 6 except for Case 4 and (c) is for the first three days.

5. Concluding remarks

The four different formulae of turbulent exchanges of heat and momentum were examined in this paper. If an appropriate value of the drag coefficient is given for the land and the sea, we can represent a difference in intensity between the land and the sea breezes. In that case, corresponding to the fluxes in the surface layer, it is necessary for the formula of turbulent exchanges in the transition layer to take into consideration the stratification and the wind shear.

Case 2 represents some properties which have been pointed out as characteristics

of the land and sea breeze. Although there remains some uncertainty in the vertical profile of K and its values, we may take this formula as an adequate approximation.

The land and sea breeze obtained in Case 3 shows some peculiar properties. An excessive intensity of the counter flow in upper levels is a decisive defect which is probably associated with excessively large values of K in the lower portion of the transition layer.

The use of the formula by which K is calculated locally from the distributions of temperature and wind yields very small values of K and consequently a very weak sea breeze circulation. In Cases 2 and 3 an enhancement of unstable stratification in the surface layer results in increasing the value of K in upper levels at which the stratification is stable. This situation can be interpreted as an effect of the so-called "penetrative convection". A local evaluation of K such as in Case 4 does not allow the effect directly. Meanwhile, the use of the formula in Case 4 in which K is proportional to the vertical wind shear results in a small value of K due to a small shear associated with the land and sea breeze and subsequently an extremely weak development of the land and sea breeze. It is important to establish a scheme parameterizing penetrative convections, and the stratification parameter α in the formula of K remains to be re-examined.

Acknowledgments

This work was financially supported by Funds for Scientific Research from the Ministry of Education. Numerical computations were made with the use of the FACOM 230-60 computer at the Data Processing Center of Kyoto University.

References

- Blackadar, A. K., 1962; The vertical distribution of wind and turbulent exchange in a neutral atmosphere, *J. Geophys. Res.*, **67**, 3095-3102.
- Defant, F., 1951; Local winds, in *Compendium of Meteorology*, Amer. Meteor. Soc., Boston, 655-672.
- Estoque, M. A., 1961; A theoretical study of the sea breeze, *Quart. J. R. Meteor. Soc.*, **87**, 136-146.
- , 1962; The sea breeze as a function of the prevailing synoptic situation; *J. Atmos. Sci.*, **19**, 244-250.
- , 1963; A numerical model of the atmospheric boundary layer, *J. Geophys. Res.*, **68**, 1103-1113.
- , and M. Bhumralkar, 1969; Flow over a localized heat source, *Month. Weath. Rev.*, **97**, 850-859.
- Haurwitz, B., 1947; Comments on the sea-breeze circulation, *J. Meteor.*, **4**, 1-8.
- Magata, M., 1965; A study of the sea breeze by the numerical experiment, *Pap. in Meteor. Geophys.*, Tokyo, **16**, 23-26.
- McPherson, R. D., 1970; A numerical study of the effect of a coastal irregularity on the sea breeze, *J. Appl. Meteor.*, **9**, 767-777.
- Neumann, J. and Y. Mahrer, 1971; A theoretical study of the land and sea breeze circulation, *J. Atmos. Sci.*, **28**, 532-542.
- O'Brien, J. J., 1970; Note on the vertical structure of the eddy exchange coefficient in the planetary

- boundary layer, *J. Atmos. Sci.*, **27**, 1213–1215.
- Schmidt, F. H., 1947; An elementary theory of the land- and sea-breeze circulation, *J. Meteor.*, **4**, 9–15.
- Zilitinkevich, S. S., D. L. Laikhtman and A. S. Monin, 1967; Dynamics of the atmospheric boundary layer, *Izv., Atmos. Ocean. Phys.*, **3**, 297–333.